

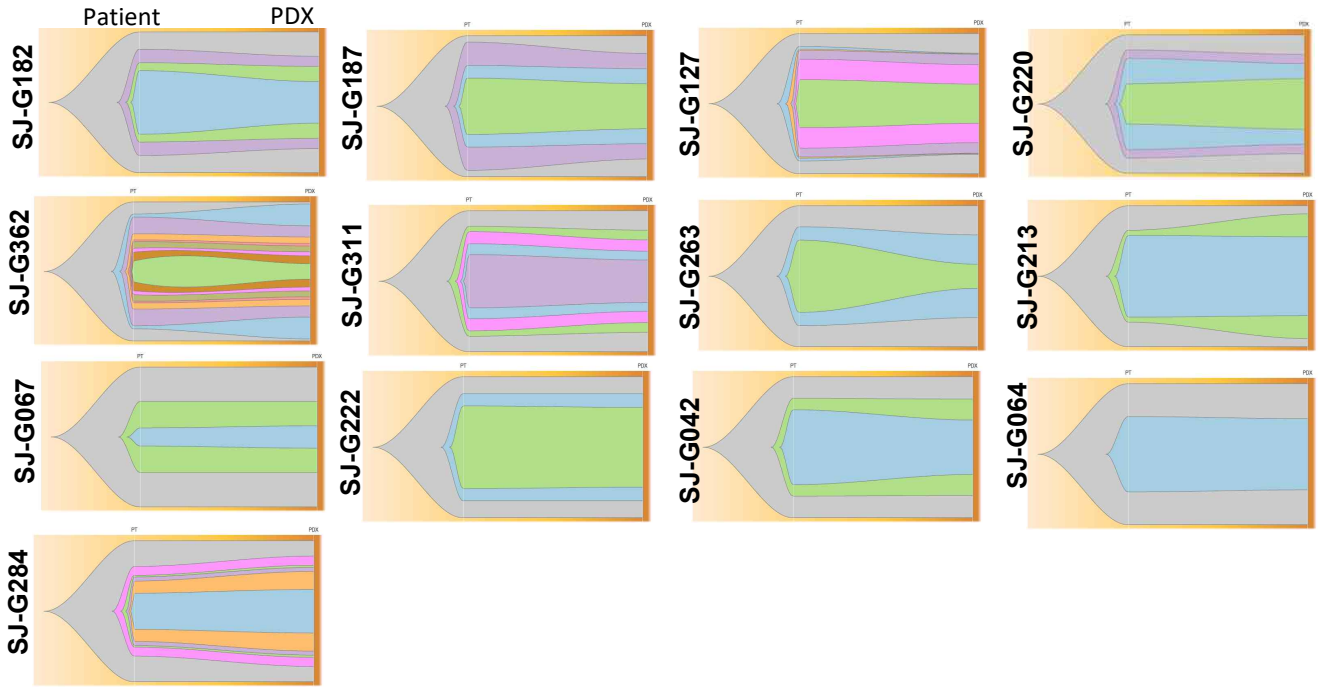
## **Supplementary Figures & Tables**

### **Predictive biomarkers for 5-fluorouracil and oxaliplatin-based chemotherapy in gastric cancers via profiling of patient-derived xenografts**

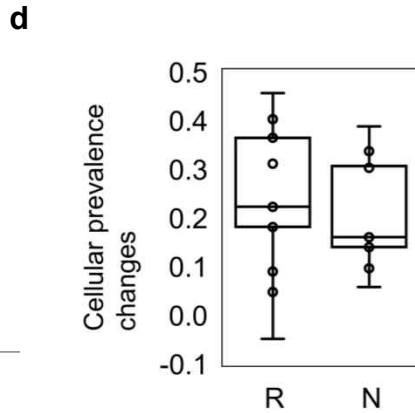
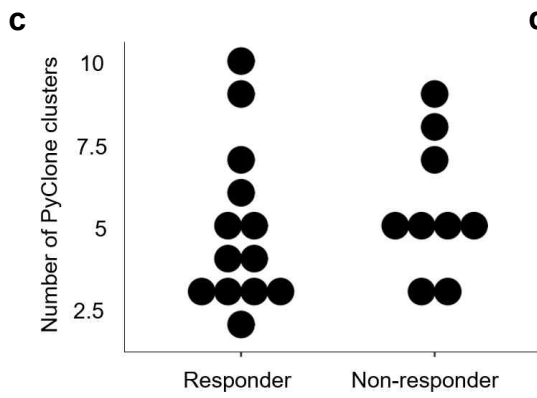
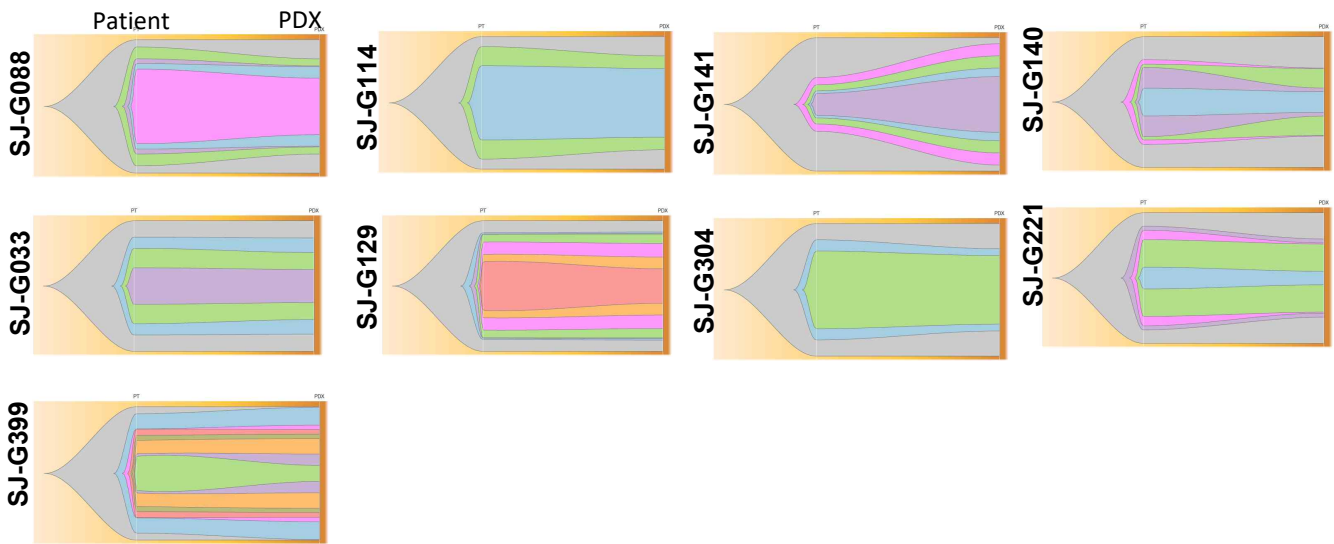
Deukchae Na, Jeessoo Chae, Sung-Yup Cho, Wonyoung Kang, Ahra Lee, Seoyeon Min, Jinjoo Kang, Min Jung Kim, Jaeyong Choi, Woochan Lee, Dongjin Shin, Ahrum Min, Yu-Jin Kim, Kyung-Hun Lee, Tae-Yong Kim, Yun-Suhk Suh, Seong-Ho Kong, Hyuk-Joon Lee, Woo-Ho Kim, Hansoo Park, Seock-Ah Im, Han-Kwang Yang, Charles Lee, and Jong-Il Kim



**a Responder**



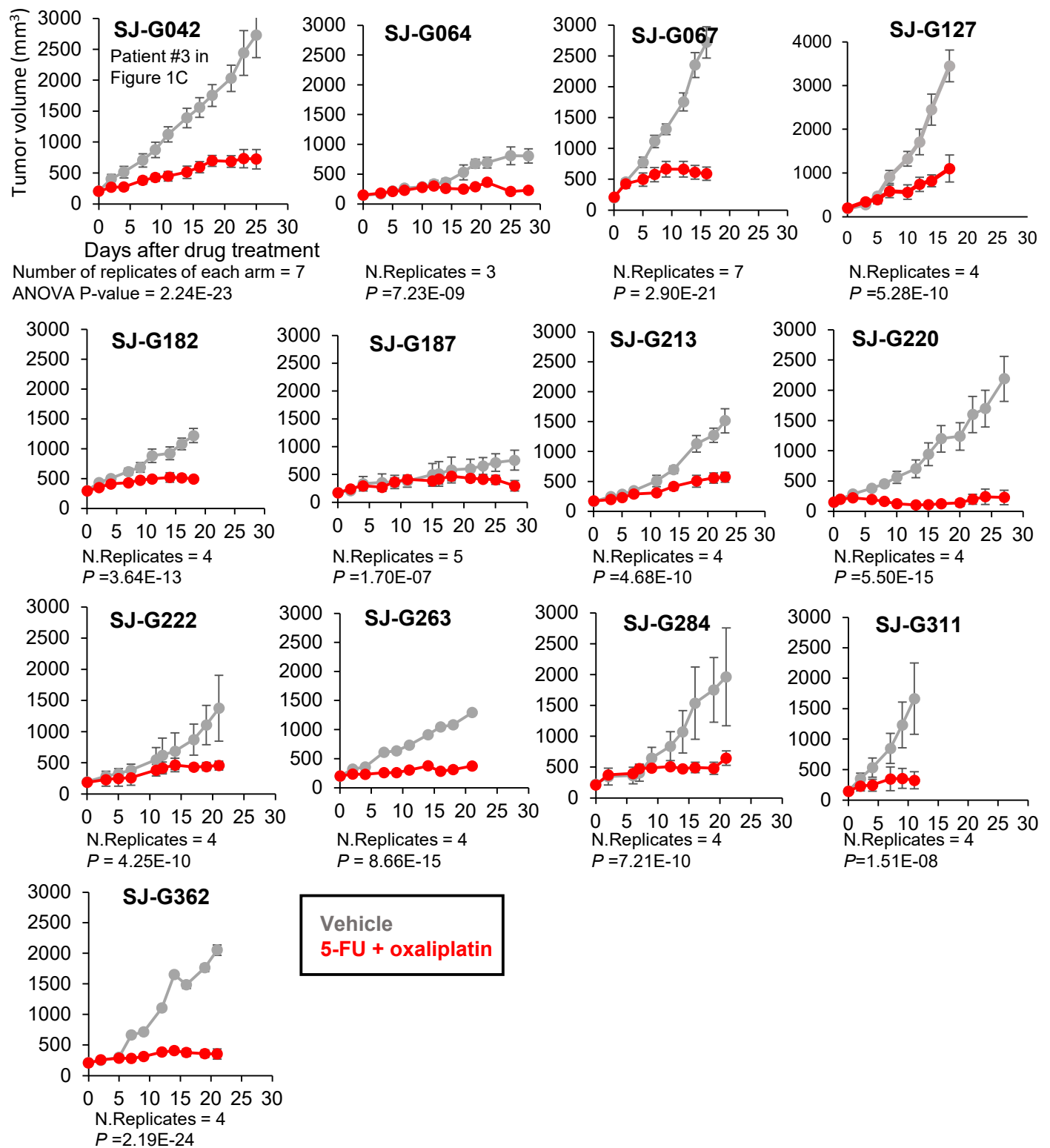
**b Non-responder**



**Supplementary Figure 2. Clonal structure analysis using whole exome sequencing data.**

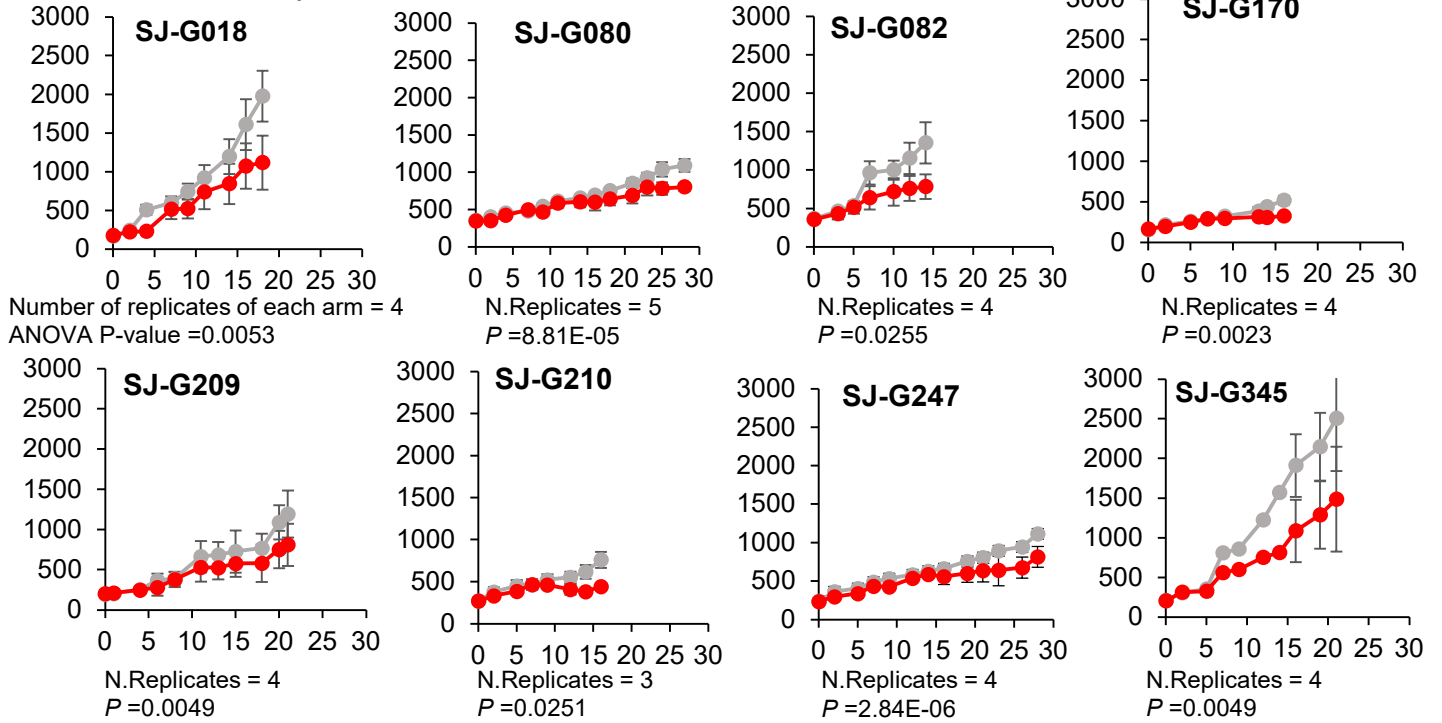
**a, b**, Changes in clonal structures between patient and PDX tumors inferred by PyClone in responder (n=13) and non-responder (n=9; excluding two samples with low number of mutations) groups. **c**, Number of Pyclone clusters (n=13 for responder, n=9 for non-responder). **d**, Cellular prevalence of changes between patient and PDXs in responder (R) and non-responder (NR) groups (n=13 for responder, n=9 for non-responder). Box plot were presented as median value and standard deviation. The bottom and top edges of the box indicate the 25th and 75th percentiles, respectively.

**a Responder**

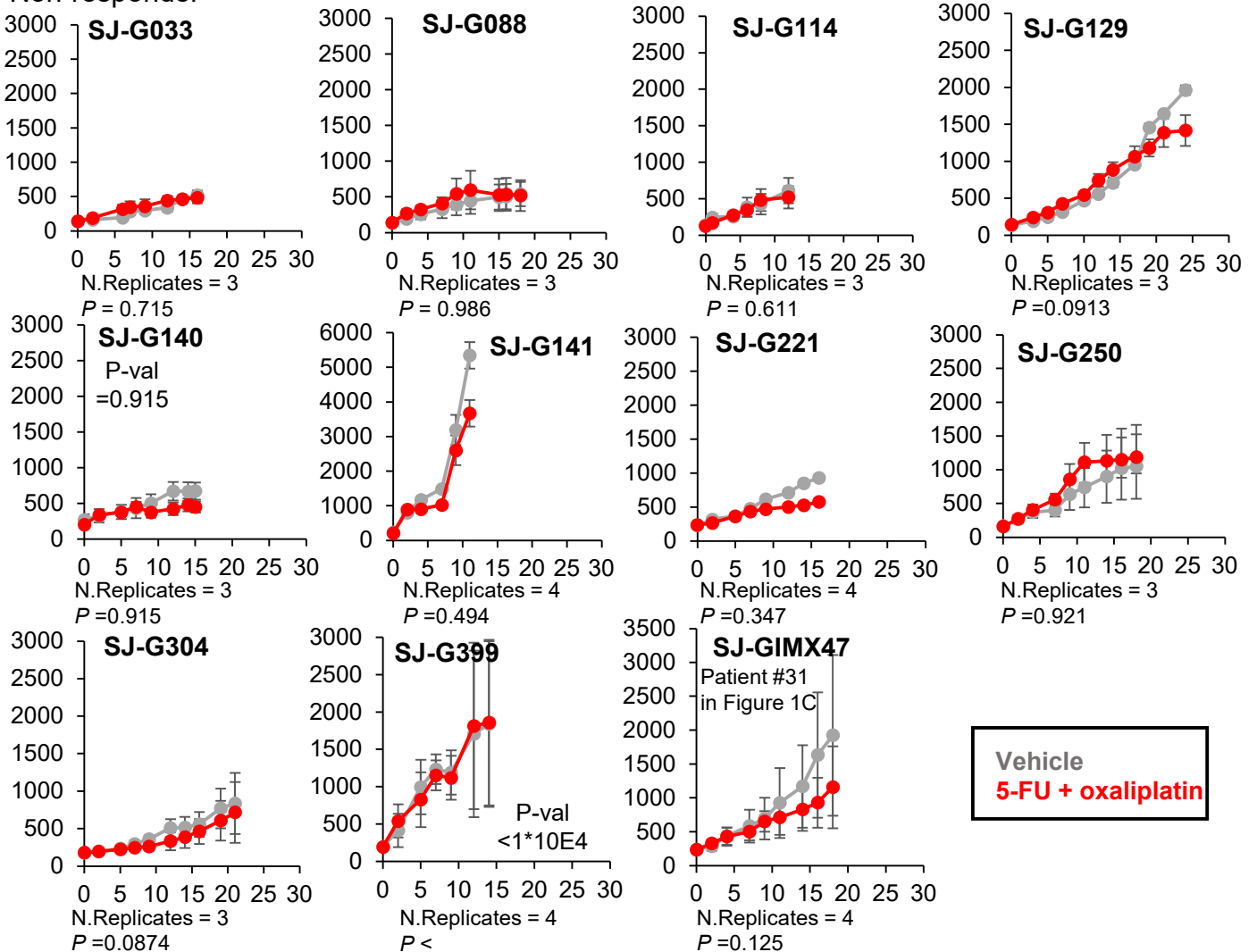


**Supplementary Figure 3. 5-FU + oxaliplatin response screening test in 32 GC PDX models. a-c,** Tumor growth curves of average volume of 5-FU + oxaliplatin treatment and vehicle groups are shown; a, responder, b, intermediate responder and c, non-responder. Data are presented as mean value and standard deviation. Two-way ANOVA with replication. Tumor growth observation data used in (a)-(c) were provided in Source Data.

**b Intermediate responder**

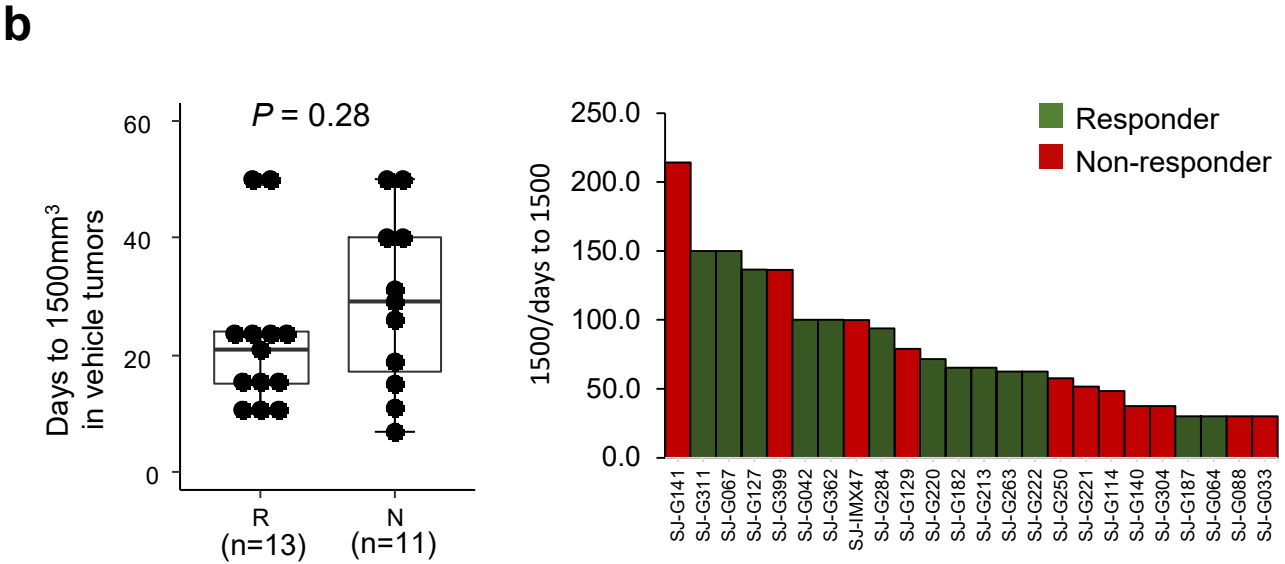
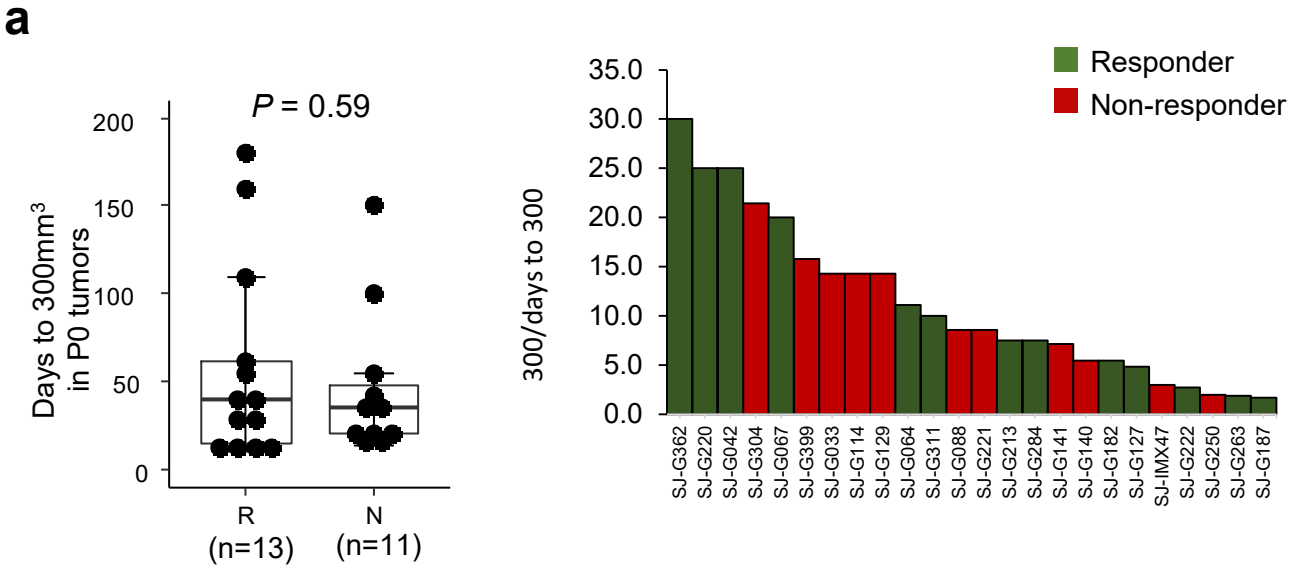


**c Non-responder**

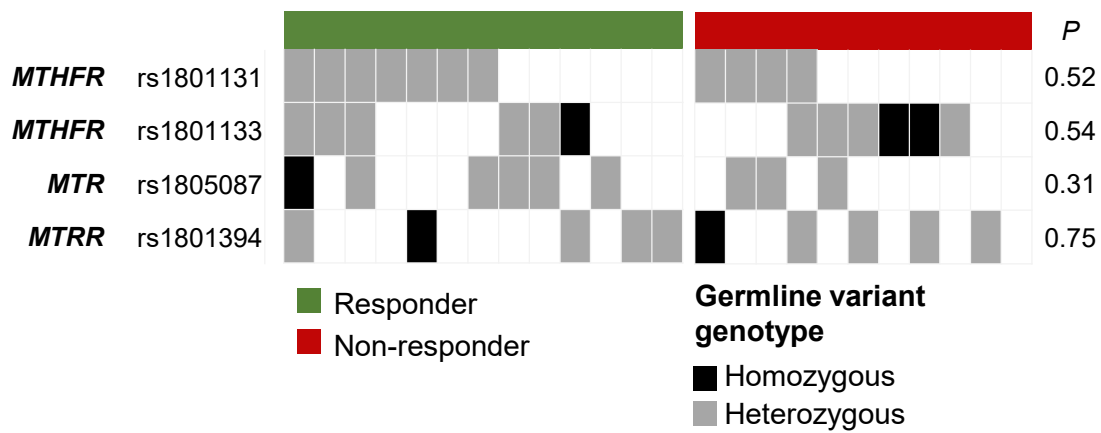
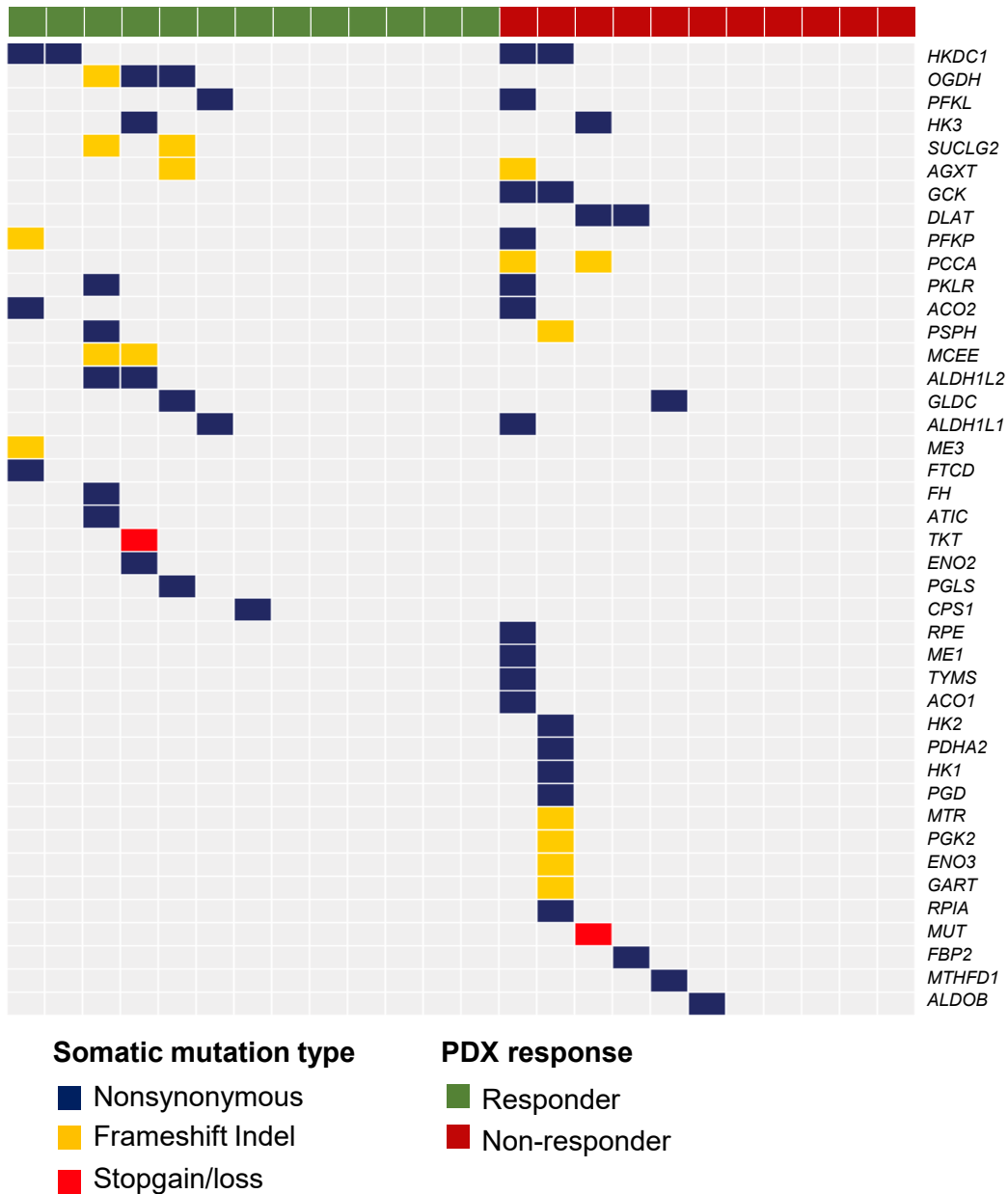


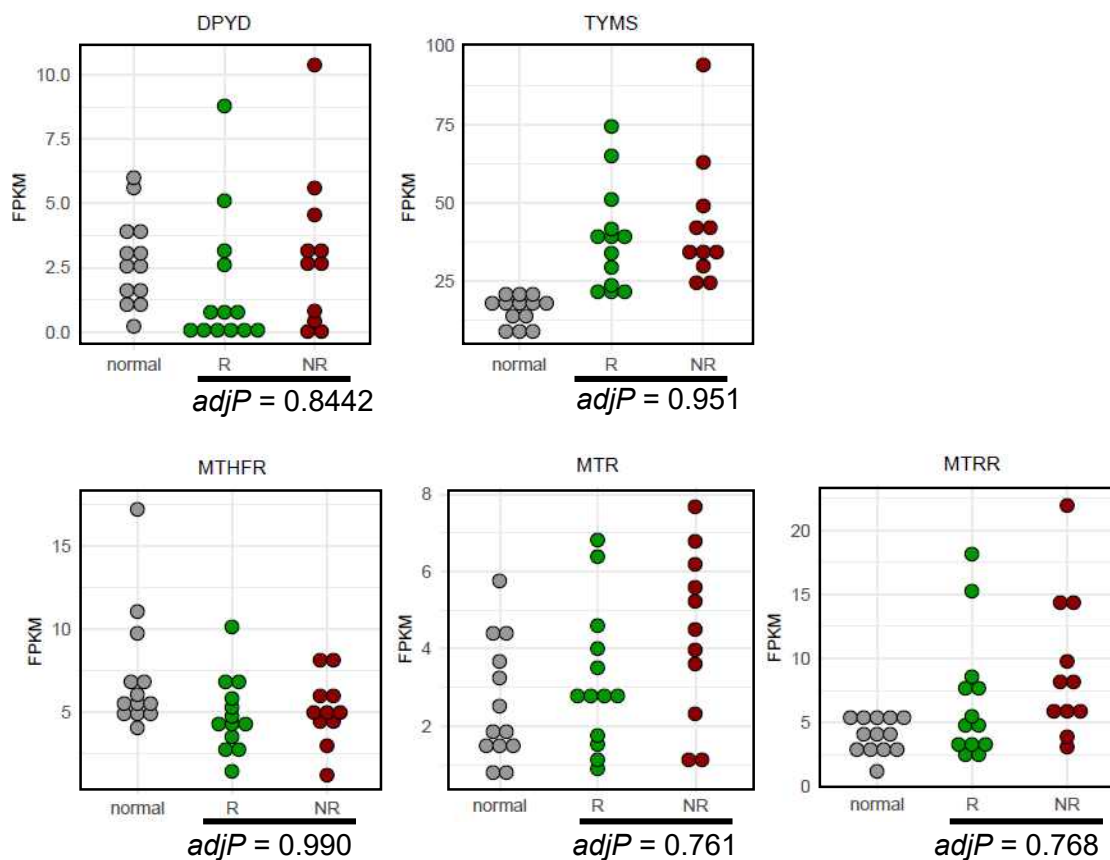
**Vehicle**  
**5-FU + oxaliplatin**

**Supplementary Figure 3 (continued).**

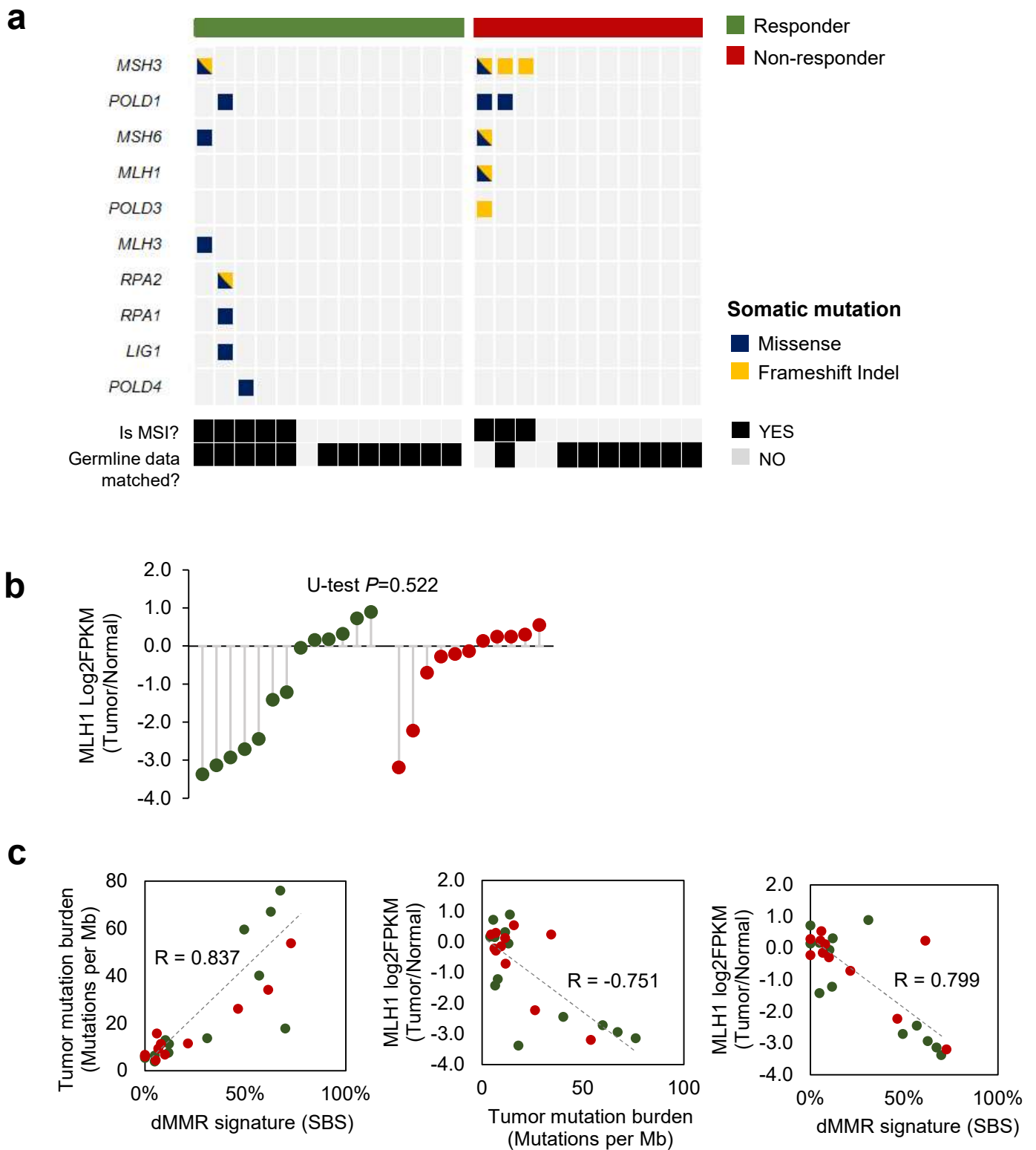


**Supplementary Figure 4. Comparison of the number of days that tumor volume reaches a certain size. a,b**, Number of days for tumor volume reaching 300 mm<sup>3</sup> during the patient-to-PDX engraftment (P0; a) and 1500 mm<sup>3</sup> in a vehicle group during screening test (b). Box plot were presented as median value and standard deviation. The bottom and top edges of the box indicate the 25th and 75th percentiles, respectively. Two-sided Student's T-test was performed. Tumor growth rate between the response and non-response groups was not significantly different.

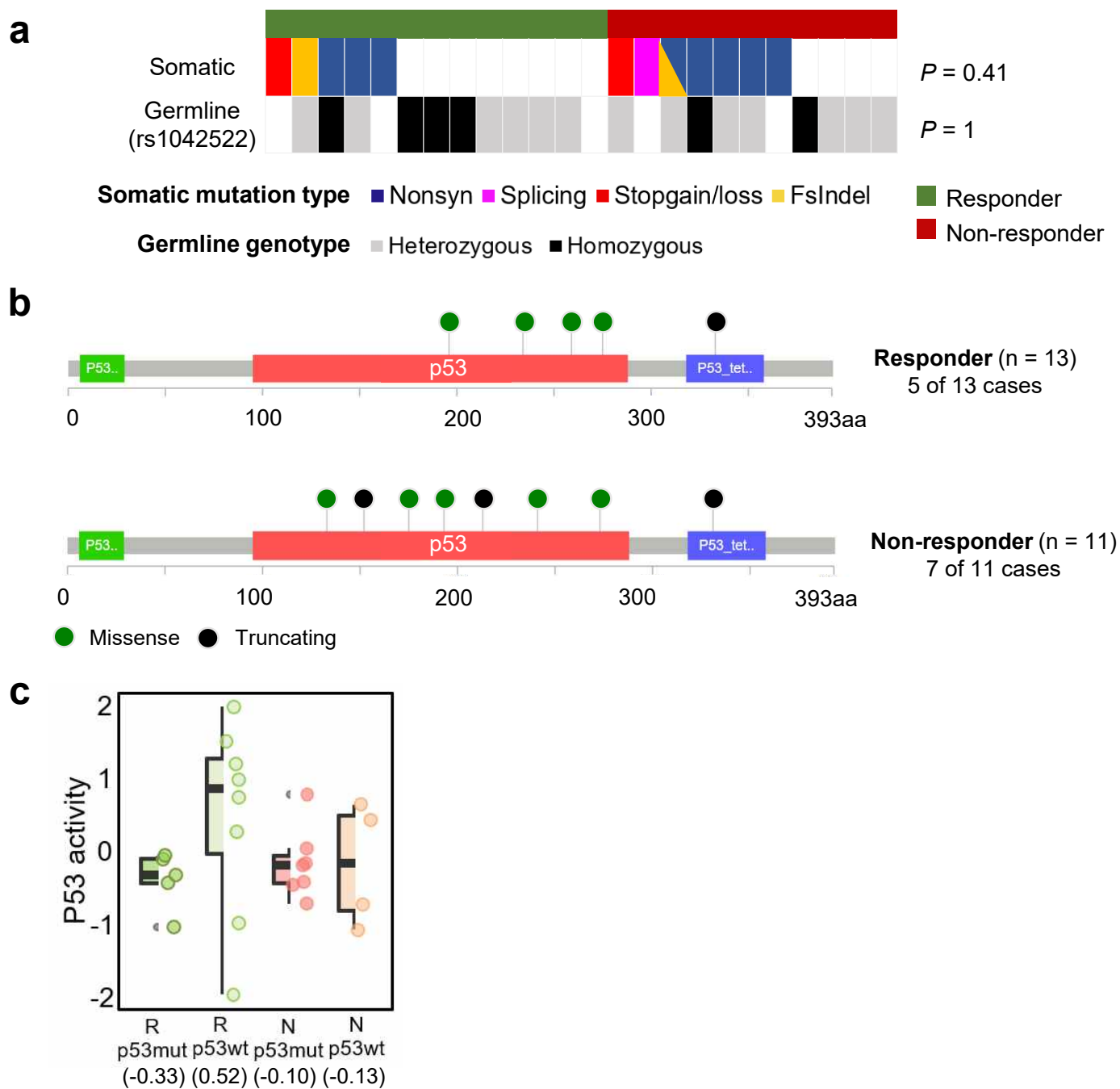
**a****b**

**C**

**Supplementary Figure 5. Mutational profiles and dysregulation pattern of one-carbon metabolism (OCM) pathway.** a, Germline variant status of previously reported genes and variants which might be related to 5-FU metabolism. Allele frequency of R and NR didn't show significant difference between two groups. Two-sided Fisher's exact test for P-values. b, Mutation profiles on carbon metabolism and one carbon pool by folate gene sets based on KEGG database. c, Gene expression of 5-FU metabolism associated genes was not significant. P-values attained by the Wald test corrected for multiple testing.

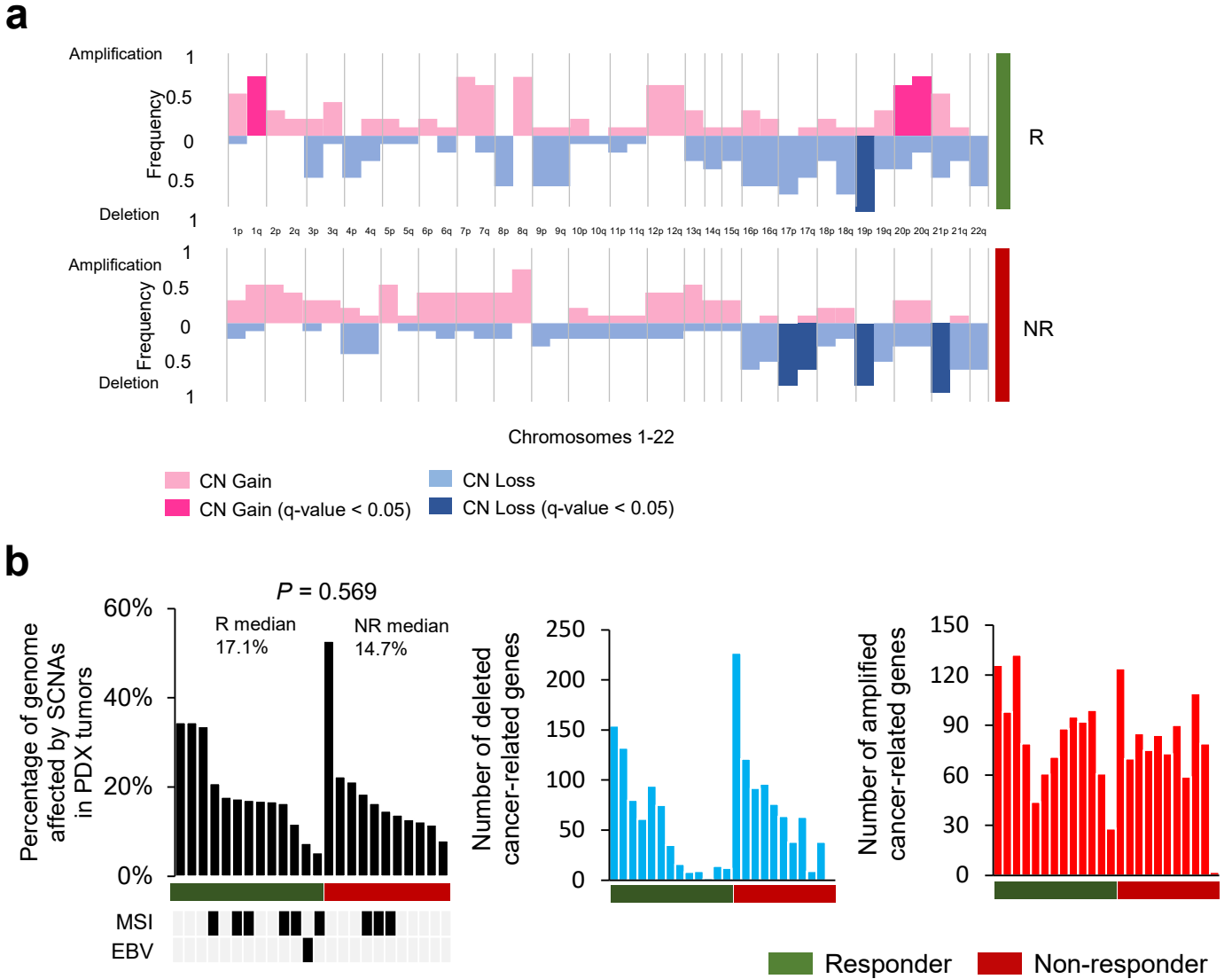


**Supplementary Figure 6. Alterations of genes in mismatch repair (MMR) pathway based on KEGG gene-set. a**, Mutational profiles of MMR pathway genes in PDX tumors. **b**, Gene expression profiles of *MLH1* in PDX tumors. Two-tailed Mann-whitney U test for P-value. **c**, Correlation of tumor mutation burden, defective MMR signature, and *MLH1* expression.

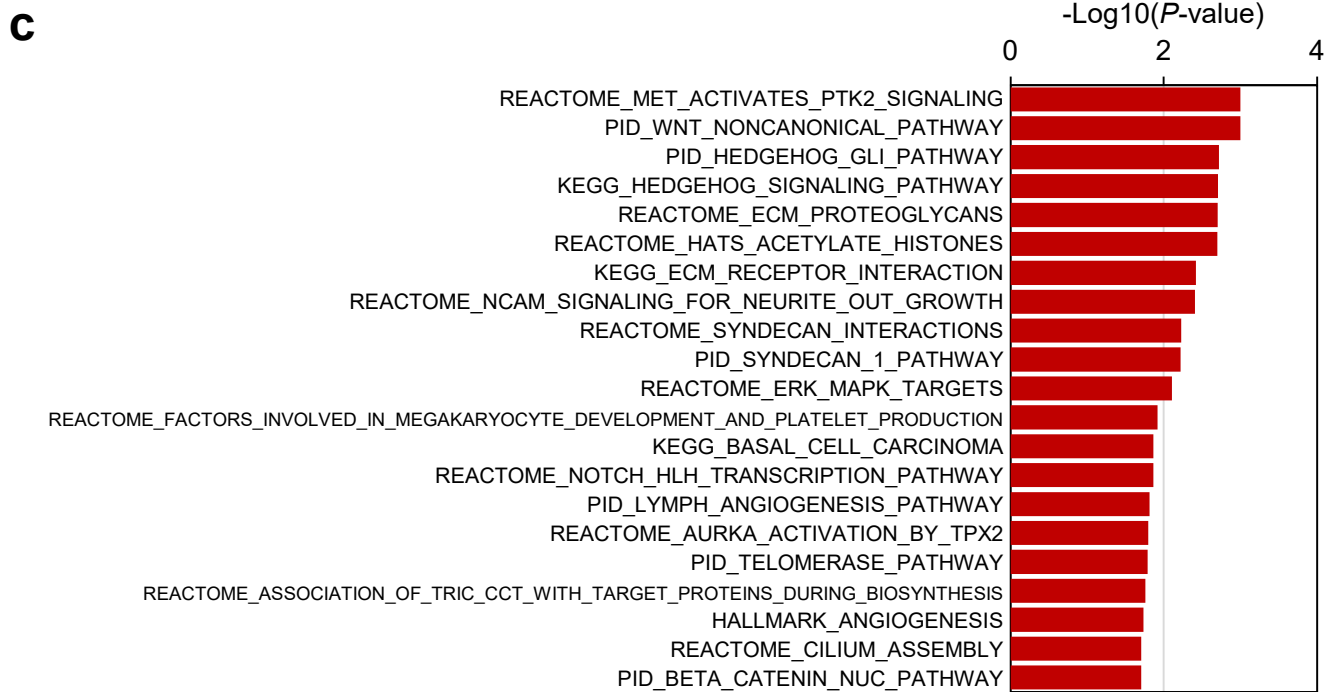
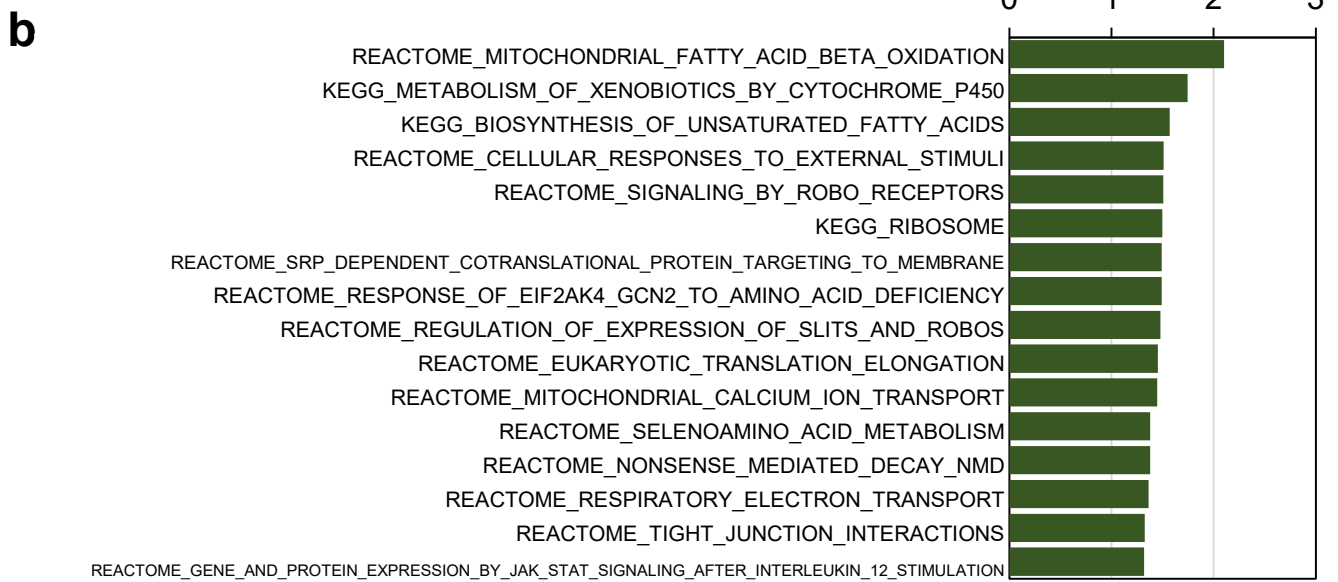
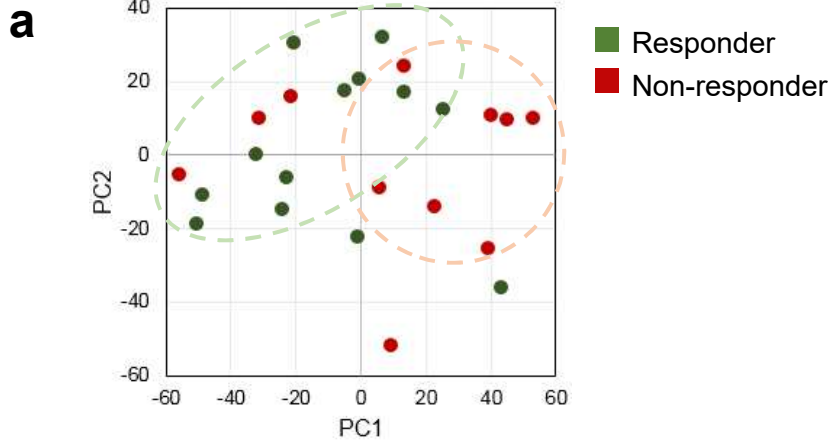


**Supplementary Figure 7. Mutational profiles of *TP53* gene and p53-activity signature. a,**

Overall somatic mutation status and drug-response related germline variant (rs1042522, ClinVar accession: VCV000012351) of *TP53*. Nonsyn: nonsynonymous, FsIndel: frame-shift insertion or deletion. Two-sided Fisher's exact test for P-values. **b,** The p53 protein domains affected by somatic mutations. **c,** p53-activity signature calculated by taking average of FPKM values from *MDM2* and *CDKN1A*, which are p53 transcriptional targets. Non-responder showed low p53 activity regardless of *TP53* mutation status. R: responder, N: non-responder.

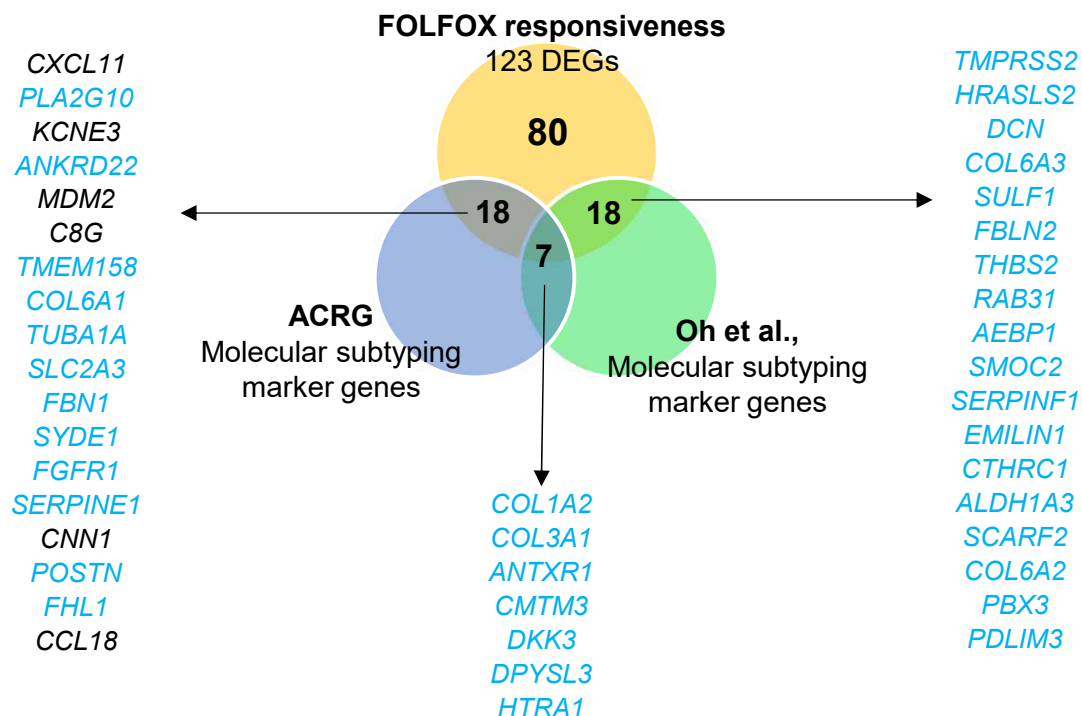


**Supplementary Figure 8. Somatic copy number alterations (SCNAs) in PDX tumors. a,** SCNAs of PDX tumors in chromosome levels of 13 R and 11 NR, estimated using whole exome sequencing data. False Discovery Rate (FDR) q-values calculated by GISTIC algorithm. **b,** PDX tumor genome affected by SCNAs (left), deletion (middle), and amplification (right) in responder (n=13) and non-responder (n=11) groups. Two-tailed Mann-Whitney U test ( $P=0.5691$ ).

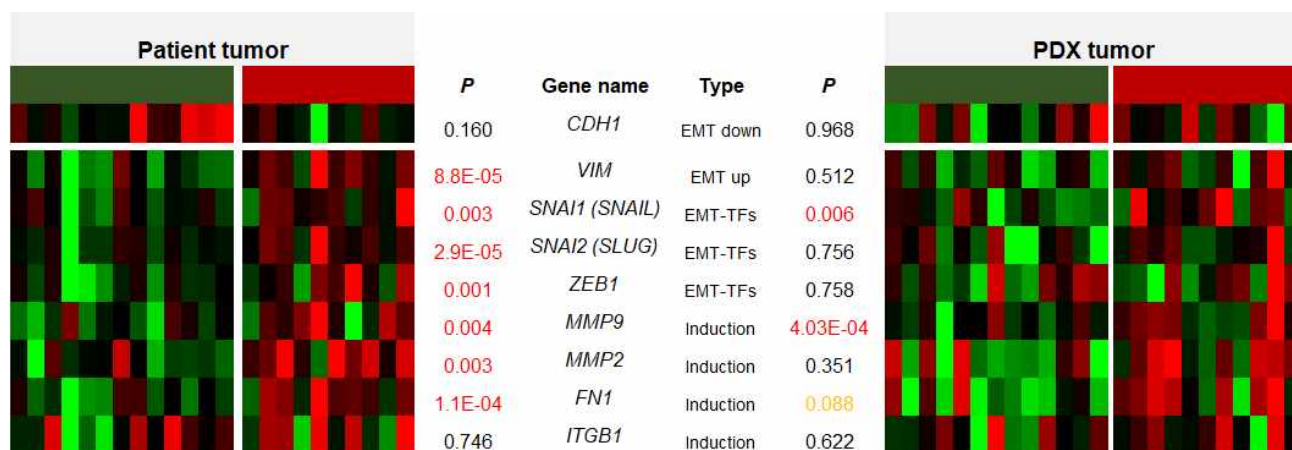


**Supplementary Figure 9. Transcriptome analyses of PDX tumors.** **a**, Principal component analysis of RNA sequencing data of PDX tumors from responder and non-responder groups. **b**, Significantly enriched gene sets in significantly up-regulated genes in responder group PDXs compared to non-responder group PDXs. Nominal P-values from GSEA. **c**, Significantly enriched gene sets in significantly up-regulated genes in non-responder group PDXs compared to responder group PDXs. Nominal P-values from GSEA.

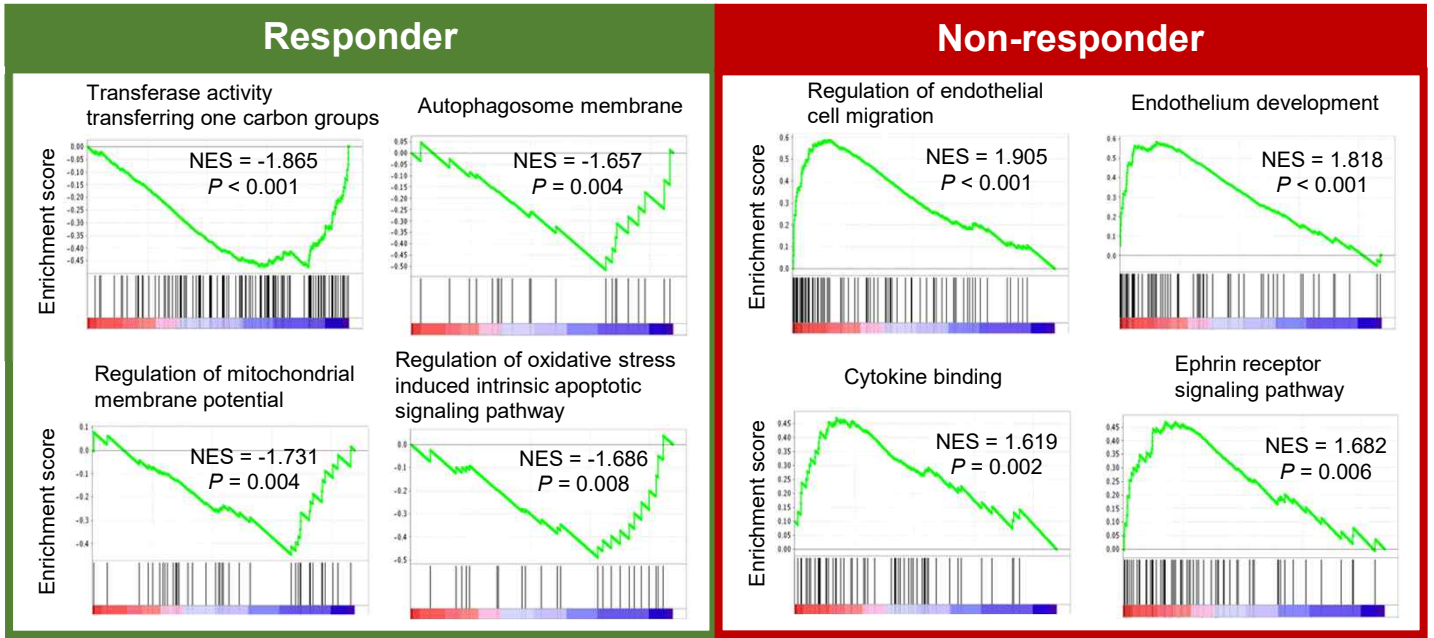
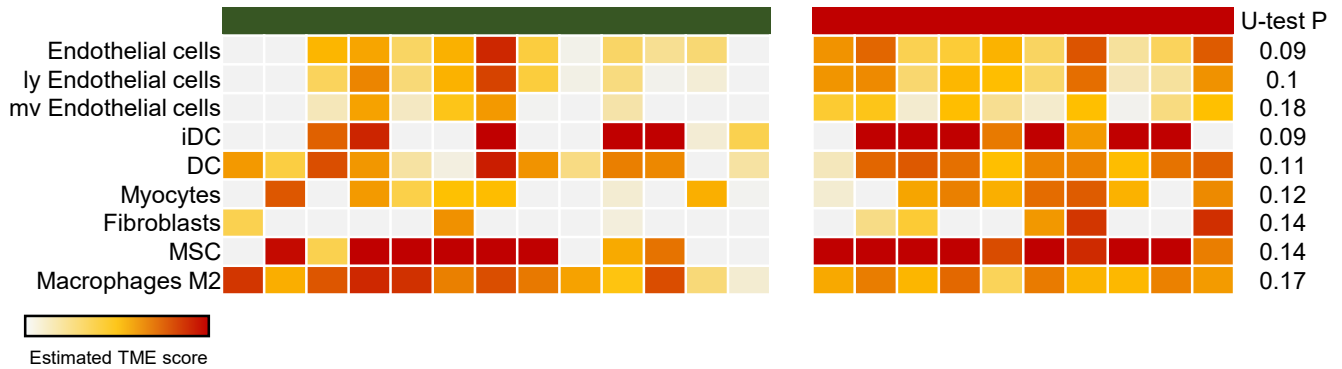
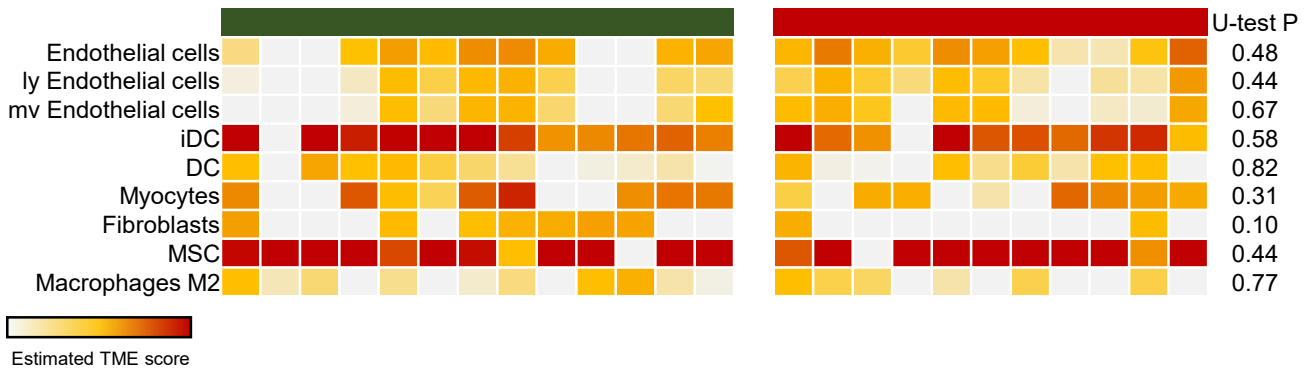
**a**

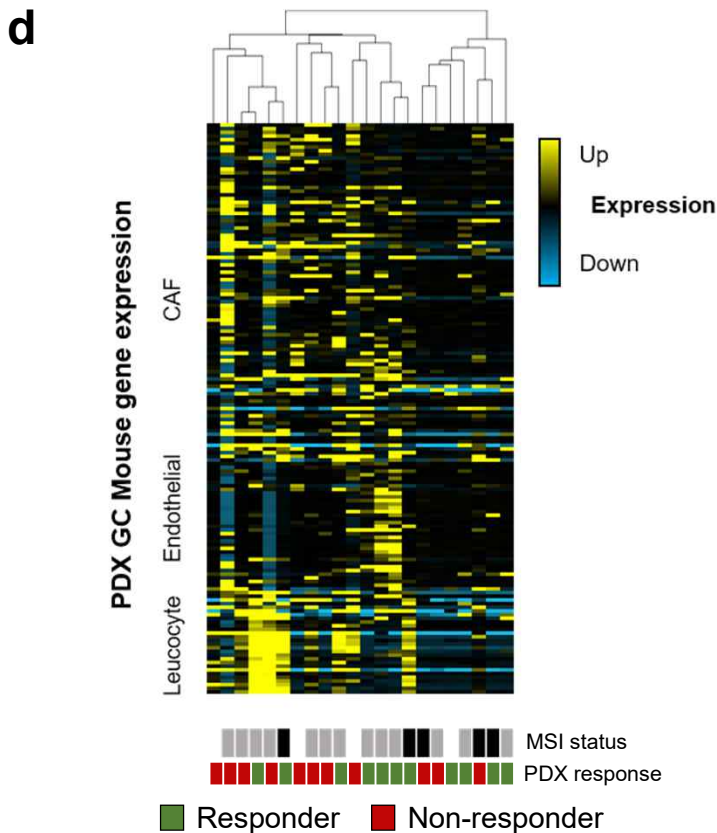


**b**

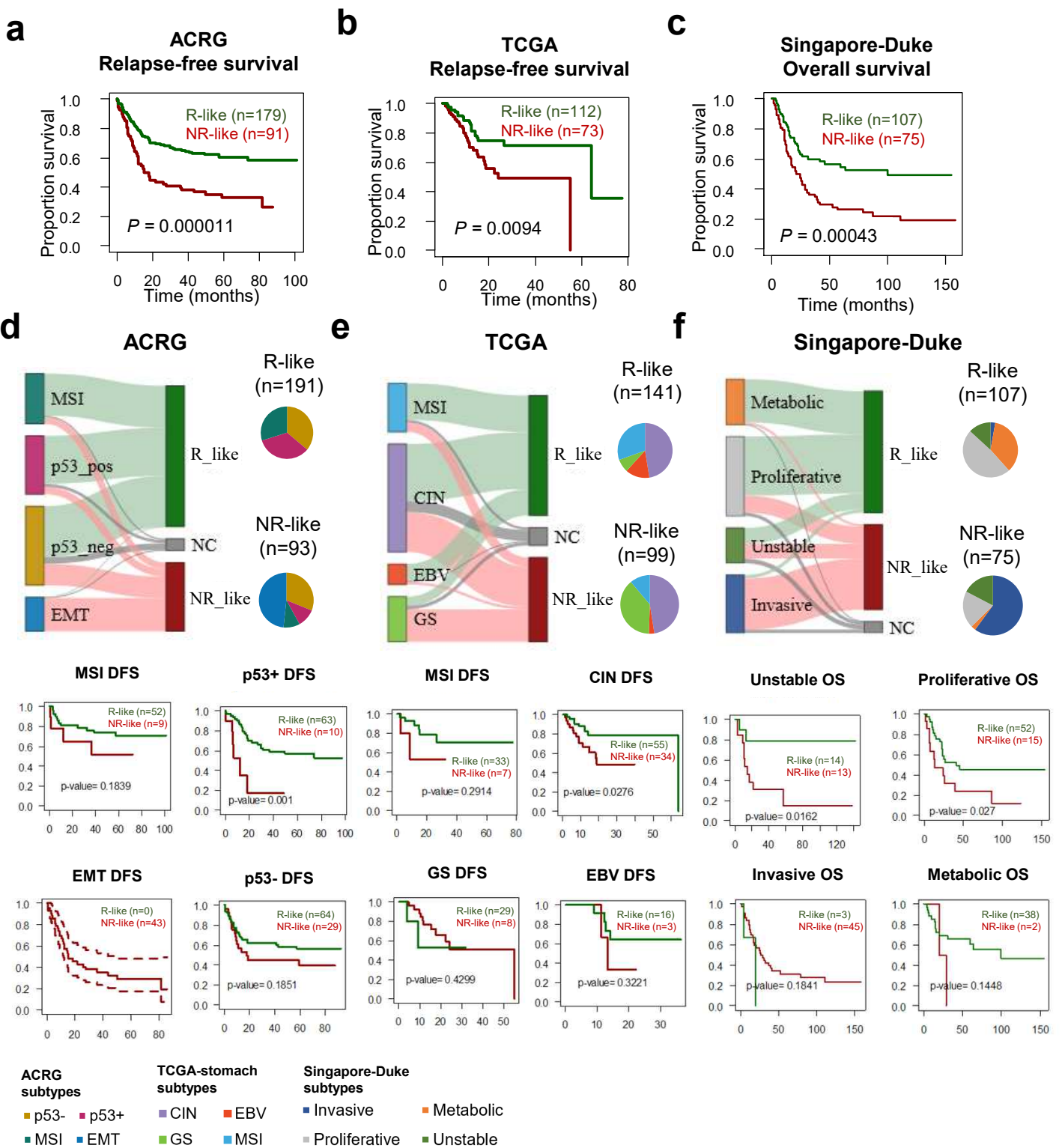


**Supplementary Figure 10. Expression of EMT-related genes in PDX models. a**, Venn diagram of overlapping genes with previously reported molecular subtyping markers of gastric cancer. Differentially expressed genes between responder and non-responder largely included mesenchymal/EMT-associated genes (genes up-regulated in mesenchymal/EMT are colored in blue). **b**, EMT marker genes are significantly up-regulated in non-responder. EMT-TF: Transcription factor in EMT. Two-sided Wald test for *P*-value.

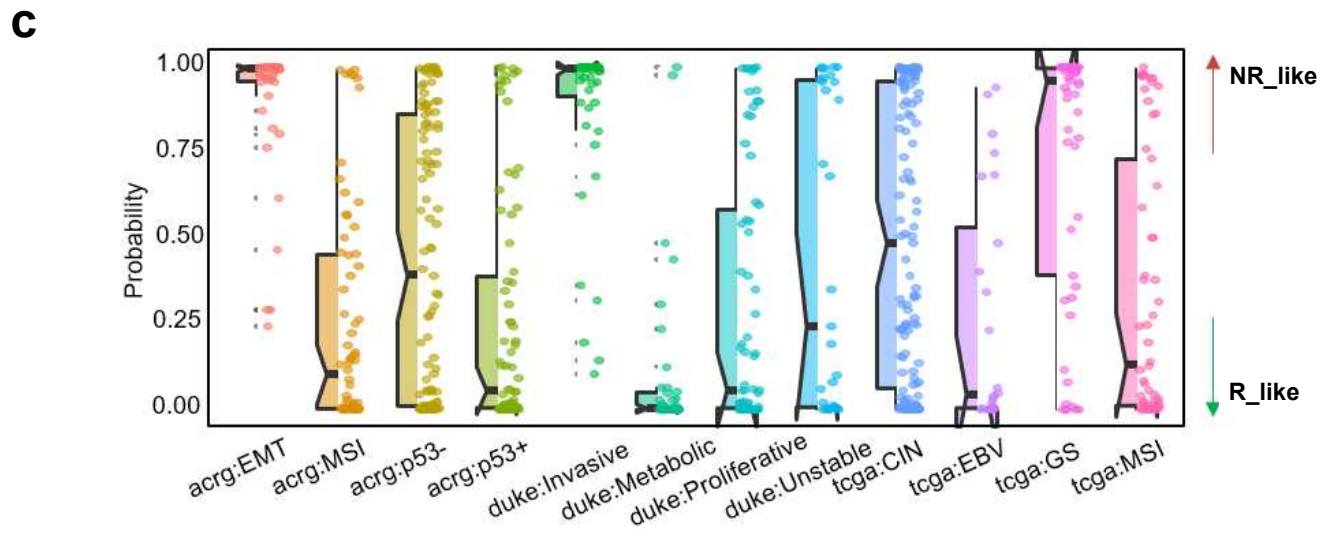
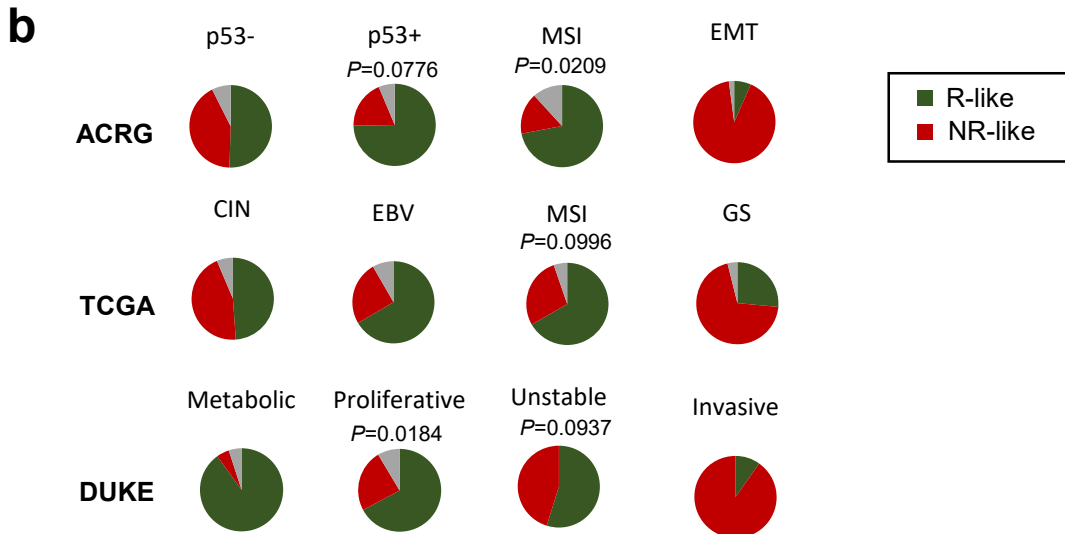
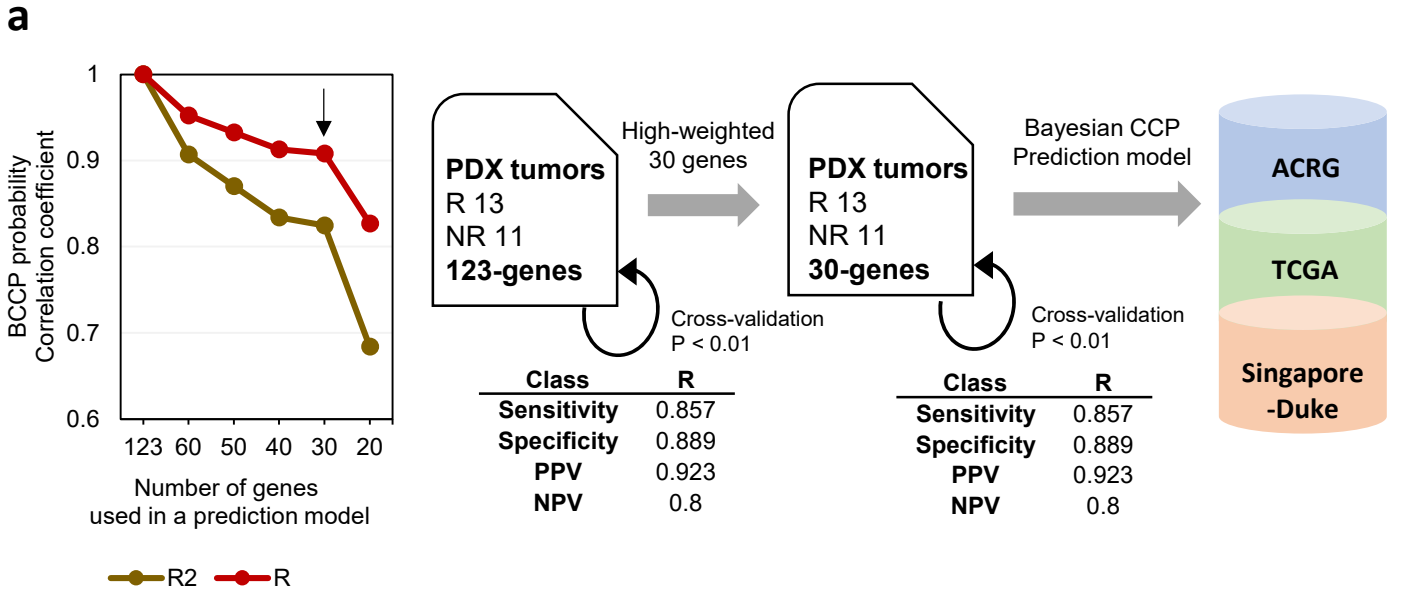
**a****b** Patient tumor TME**c** PDX tumor TME



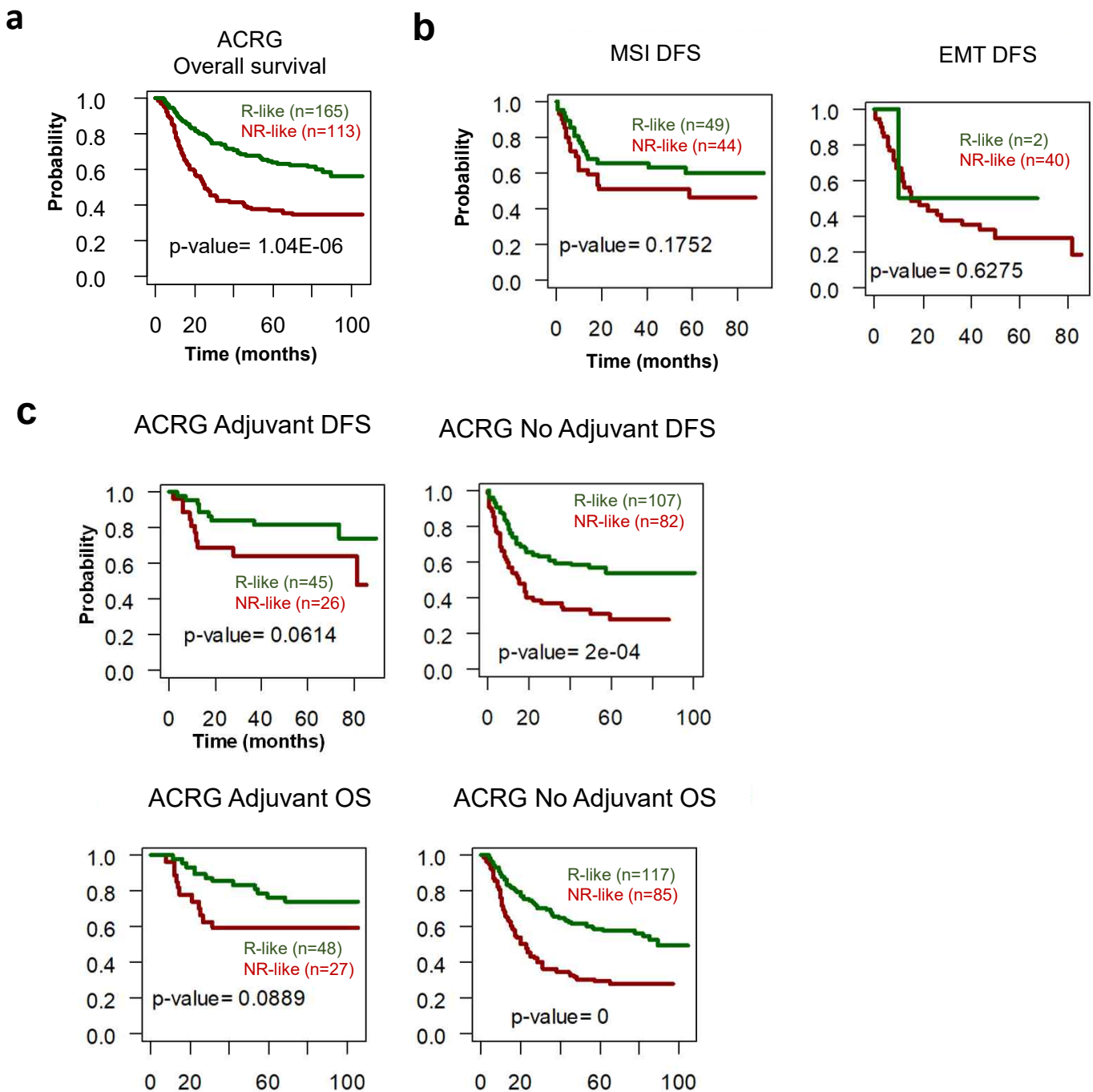
**Supplementary Figure 11. Transcriptome analysis of tumor microenvironment in responder and non-responder groups.** **a**, Gene set enrichment analysis of tumor microenvironment inferred by mouse-specific gene expression from PDX tumors, based on Gene Ontology and KEGG terms comparing responder and non-responder. **b**, Composition of stromal cells in patient tumors inferred from RNA sequencing data using xCell algorithm. **c**, Composition of stromal cells in PDX tumors inferred from RNA sequencing data using xCell algorithm. Two-tailed Mann-whitney U test for P values in b-c. **d**, Unsupervised clustering of gene expression in responders and non-responders based on a set of marker genes associated with stromal cells, such as cancer-associated fibroblasts (CAFs), endothelial cells and leucocytes.



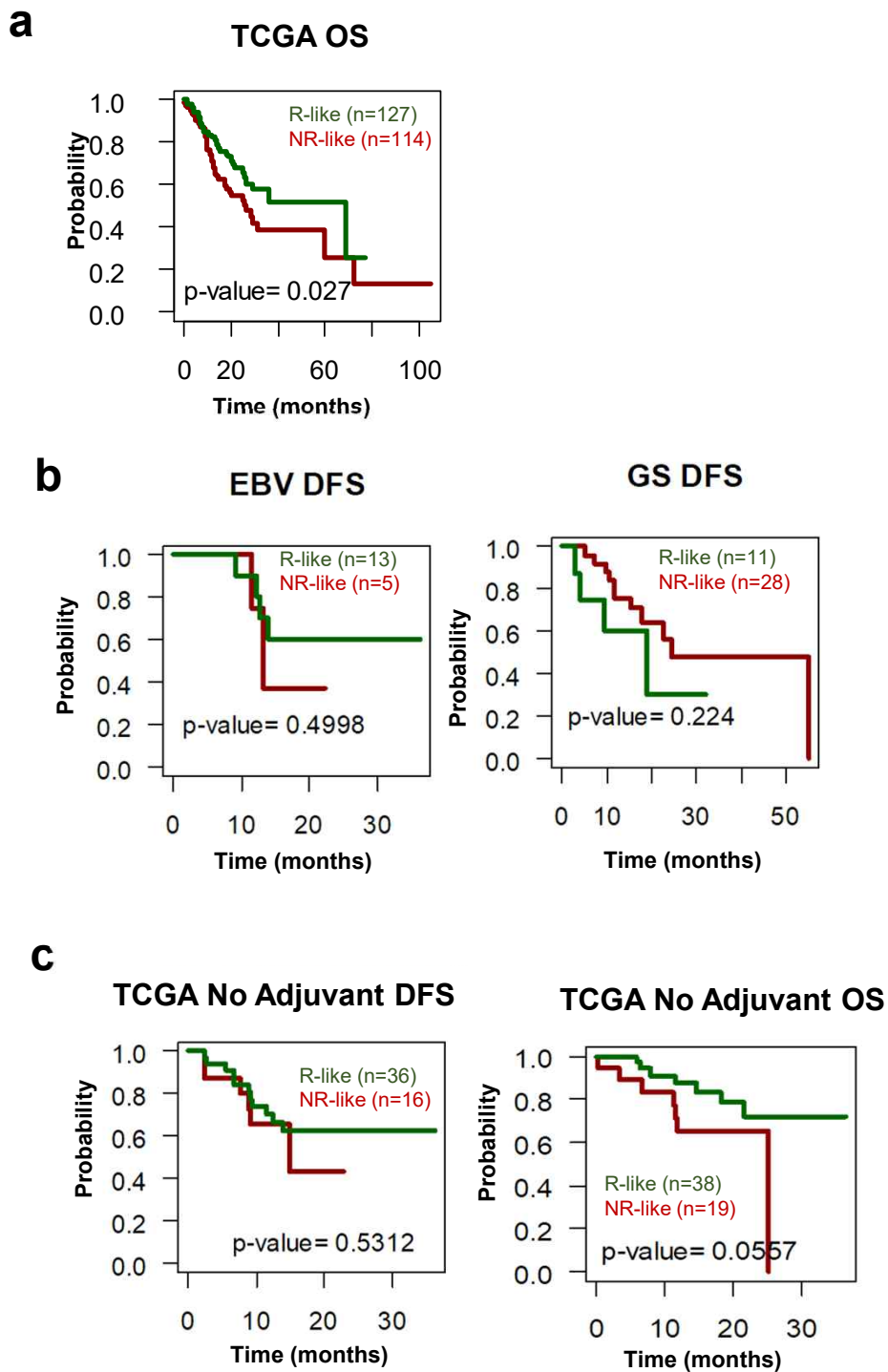
**Supplementary Figure 12. Initial 5-FU + oxaliplatin response prediction model developed using 123 DEGs.** **a-c**, Survival analyses for GC patients in ACRG (a), TCGA (b), and Singapore-Duke (c) studies, according to prediction model. Patients were stratified by our prediction model, and the responder-like (R-like) patient group showed a significantly better prognosis than the non-responder-like (NR-like) group with a 123-gene prediction model. P-values were calculated from the log-rank test. ACRG: the Asian Cancer Research Group. **d-f**, Reassignment of GC patients from the ACRG study (d), TCGA (e), and Singapore-Duke (f) studies according to prediction model (Top). Survival analyses for subgroups in ACRG (d), TCGA (e), and Singapore-Duke (f) studies, according to prediction model (bottom). P-values were calculated from the two-sided log-rank test. p53+ group of ACRG cohort, CIN group of TCGA cohort and Unstable and Proliferative groups of Singapore-Duke cohort showed significant differences in survival between R-like and NR-like groups.



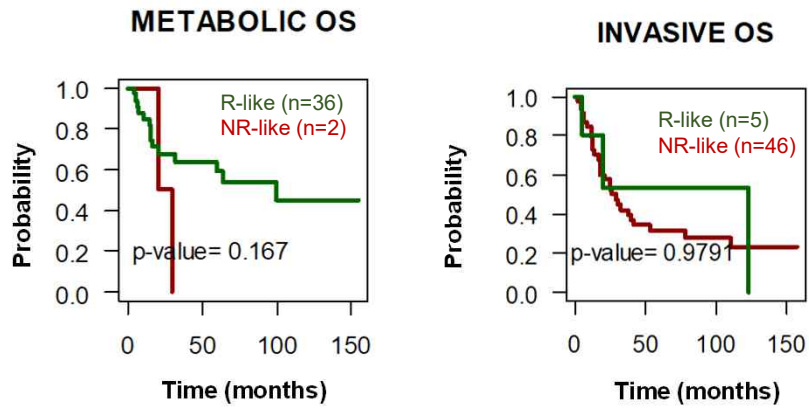
**Supplementary Figure 13. Building a 30-gene 5-FU + oxaliplatin responsiveness prediction model.** **a**, Development of predictive model applying Bayesian CCP (BCCP) algorithm and selection of the minimum number of genes in the predictive model. **b**, The proportion of predicted results of 5-FU + oxaliplatin responsiveness by molecular subtypes based on 30-gene model. Two-sided log-rank test between R-like and NR-like groups for difference in survival. **c**, The BCCP probability of each patient in validation cohorts by molecular subtypes.



**Supplementary Figure 14. Survival analysis of Asian Cancer Research Group (ACRG) GC patients reclassified by our 30-gene response prediction model. a,** Patients were stratified by our prediction model in responder-like (R-like) and non-responder-like (NR-like), and overall survival was compared between two groups. **b,** Disease-free survival (DFS) and overall survival (OS) analyses between R-like and NR-like patients in each molecular subtype of ACRG study. **c,** DFS and OS analysis of patients regarding the chemotherapy status. Two-sided log-rank test was performed for *P*-values in (a)-(c).



**Supplementary Figure 15. Survival analysis of TCGA study GC patients reclassified by our 30-gene response prediction model. a,** Patients were stratified by our prediction model as responder-like (R-like) and non-responder-like (NR-like). OS was compared using two-sided log-rank test. **b,** DFS was compared between R-like and NR-like patients by each molecular subtype of TCGA study. Two-sided log-rank test for (b)-(c). **c,** DFS and OS were compared regarding patients' adjuvant chemotherapy status.



**Supplementary Figure 16. Survival analysis of Singapore-Duke study GC patients reclassified by our 30-gene response prediction model.** OS of patients stratified by our prediction model were analyzed by molecular subtypes of Singapore-Duke study (Two-sided log-rank test for P-value).

**Supplementary table S1. List of 31 patients underwent GC PDX generation and NGS analyses**

Patient #	PDX ID	MSI status	WHO classification	Lauren classification	TNM stage	Location	WES			WTS			Pt_response
							Blood	Patient tumor	Xenograft tumor	Patient nontumor	Patient tumor	Xenograft tumor	
#1	SNUH-JAX-G018	MSI-H	PD tub	M	IIc	lower	v		v	v		v	R
#2	SNUH-JAX-G033	MSS	MD tub	I	IIa	middle	v	v	v	v	v	v	NR
#3	SNUH-JAX-G042	MSS	MD tub	I	IIb	lower	v	v	v	v	v	v	R
#4	SNUH-JAX-G064	MSI-H					v	v	v	v	v	v	
#5	SNUH-JAX-G067	MSI-H	MD tub	I	IIa		v	v	v	v	v	v	R
#6	SNUH-JAX-G080	MSS		M	IIc	lower	v	v	v	v	v	v	NR
#7	SNUH-JAX-G082	MSI-L	PD tub	I	IIa	lower	v	v	v	v	v	v	
#8	SNUH-JAX-G088	MSS	PD tub	M	IIa	lower	v	v	v	v	v	v	
#9	SNUH-JAX-G114	MSS	PCC	D	IIb	middle	v	v	v	v	v	v	NR
#10	SNUH-JAX-G127	MSS		D	IIc	lower	v	v	v		v	v	NR
#11	SNUH-JAX-G129	MSS			IIc	lower	v	v	v	v	v	v	NR
#12	SNUH-JAX-G140	MSI-H	MD tub	I	IIa	upper		v	v		v	v	
#13	SNUH-JAX-G141	MSS	MD tub	I	IV	entire	v	v	v	v	v	v	
#14	SNUH-JAX-G170	MSI-H	MD tub	I	IIa	upper	v	v	v		v	v	
#15	SNUH-JAX-G182	MSI-H	PD tub	M	Ib	lower	v	v	v	v	v	v	
#16	SNUH-JAX-G187	MSS	PD tub	D	IIb	middle	v	v	v	v	v	v	
#17	SNUH-JAX-G209	MSI-H	PD tub	M	Ib	middle	v	v	v		v	v	
	SNUH-JAX-G210						v	v	v		v	v	
#18	SNUH-JAX-G213	MSI-H	PD tub	M	IIc		v	v	v		v	v	
#19	SNUH-JAX-G220	MSI-L	PCC		IIc	lower		v	v		v	v	R
#20	SNUH-JAX-G221	MSI-H						v	v		v	v	
#21	SNUH-JAX-G222	MSS	PD tub		IIb	upper	v	v	v	v	v	v	
#22	SNUH-JAX-G247	MSS	PCC	D	IIc	lower	v	v	v	v	v	v	
#23	SNUH-JAX-G250	MSS		I	IIa	lower	v	v	v	v	v	v	NR
#24	SNUH-JAX-G263	MSS	PD tub	D	Ib	upper	v	v	v		v	v	
#25	SNUH-JAX-G284	MSI-H	MD tub	I	IIc	lower	v	v	v		v	v	
#26	SNUH-JAX-G304	MSS	PD tub	M	IIb	lower	v	v	v	v	v	v	NR
#27	SNUH-JAX-G311	MSS	MD tub	I	IIc	lower	v	v	v		v	v	
#28	SNUH-JAX-G345	MSI-H	PD tub	I		middle	v	v	v			v	
#29	SNUH-JAX-G362	MSS	PD tub	D		lower	v	v	v		v	v	
#30	SNUH-JAX-G399	MSS	PD tub	M		lower		v	v		v	v	
#31	SNUH-JAX-IMX47	MSS					v		v			v	NR

\* PD: poorly differentiated, MD: moderately differentiated, tub: tubular adenocarcinoma, PCC: poorly cohesive carcinoma, I: intestinal, D: diffuse, M: mixed, R: responsive, NR: nonreport



**Supplementary table S3. The number of responder and non-responder by clinical characteristics.**

		<b>Responder</b>	<b>Non-responder</b>	<b>P-value</b>
<b>Gender</b>	Male	11	9	0.855
	Female	2	2	
<b>Age (median)</b>		64	60	0.104
<b>WHO</b>	MD tub	4 (36%)	3 (43%)	0.875
	PD tub	6 (55%)	3 (43%)	
	PCC	1 (9%)	1 (14%)	
<b>Lauren</b>	Intestinal	4 (40%)	4 (50%)	0.407
	Mixed	2 (20%)	3 (38%)	
	Diffuse	4 (40%)	1 (13%)	
<b>Location1</b>	Upper 1/3	2 (20%)	1 (11%)	ND
	Middle 1/3	1 (10%)	2 (22%)	
	Lower 1/3	7 (70%)	5 (56%)	
	Entire	0 (0%)	1 (11%)	
<b>Location2</b>	LC	4 (33%)	5 (56%)	0.411
	GC	0 (0%)	0 (0%)	
	AW	1 (8%)	2 (22%)	
	PW	3 (25%)	1 (11%)	
	Circular	4 (33%)	1 (11%)	
<b>TNM stage</b>	I and II	3 (27%)	0 (0%)	ND
	IIIa and IIIb	3 (27%)	6 (75%)	
	IIIc and IV	5 (45%)	2 (26%)	

\* MD: moderately differentiated, PD: poorly differentiated, tub: Tubular adenocarcinoma, PCC: poorly cohesive carcinoma, LC: lesser curvature, GC: greater curvature, AW: anterior wall, PW: posterior wall, ND: not determined

\*\* P-values from the Freeman-Halton extension of the Fisher exact probability test

**Supplementary table S4. The number of responder and non-responder by TCGA subtypes**

<i>P</i> = 0.464	<b>EBV</b>	<b>MSI</b>	<b>CIN</b>	<b>GS</b>	<b>Sample number</b>
<b>Responder</b>	1 (7.7%)	5 (38.5%)	5 (38.5%)	2 (15.4%)	13
<b>Non-responder</b>	0 (0%)	2 (18.2%)	6 (54.5%)	3 (27.3%)	11

\* *P*-values from the Freeman-Halton extension of the Fisher exact probability test

